Distribution Agreement

In presenting this thesis or dissertation as a partial fulfillment of the requirements for an advanced degree from Emory University, I hereby grant to Emory University and its agents the non-exclusive license to archive, make accessible, and display my thesis or dissertation in whole or in part in all forms of media, now or hereafter known, including display on the world wide web. I understand that I may select some access restrictions as part of the online submission of this thesis or dissertation. I retain all ownership rights to the copyright of the thesis or dissertation. I also retain the right to use in future works (such as articles or books) all or part of this thesis or dissertation.

Signature:

03/16/2016

_____ _____

SRIKANT RANGARAJU Date

Expression and functional importance of microglial Kv1.3 channels in Alzheimer's Disease

By

SRIKANT RANGARAJU

MASTER OF SCIENCE

CLINICAL RESEARCH

ALLAN I. LEVEY_____

Advisor

AMITA MANATUNGA_____

Committee Member

AMIT SHAH_____

Committee Member

Accepted:

_____

Lisa A. Tedesco, Ph.D.
Dean of the James T. Laney School of Graduate Studies

_____

Date

Expression and functional importance of microglial Kv1.3 channels in Alzheimer's Disease

By

SRIKANT RANGARAJU

M.B.B.S., Tamil Nadu MGR University, India, 2007

Advisor: ALLAN I. LEVEY, MD, Ph.D.

An abstract of

A thesis submitted to the Faculty of the
James T. Laney School of Graduate Studies of Emory University

in partial fulfillment of the requirements for the degree of
Master of Science in Clinical Research

2016

Abstract

Expression and functional importance of microglial Kv1.3 channels in Alzheimer's Disease

By Srikant Rangaraju

Alzheimer's disease (AD) is the commonest dementing illness worldwide but no disease-modifying therapy exists. Accumulation and aggregation of toxic amyloid beta (Aβ) result in neurotoxicity and neuroinflammation, both of which lead to neurodegeneration and disease progression. Recent genetic studies have suggested that the innate macrophages of the brain called microglia are the key mediators of neuroinflammation in AD. Kv1.3, a voltage-gated potassium channel expressed by microglia, is a key regulator of membrane potential, calcium signaling and neurotoxic effects of activated microglia *in-vitro* and may represent a therapeutic target for drugs that inhibit neurotoxic microglial functions in AD. However, Kv1.3 channel expression patterns in the human AD brain are currently unknown. The importance of Kv1.3 channels in Aβ-induced pro-inflammatory microglial responses is also unknown. We hypothesized that (1) Activated microglia in human AD express Kv1.3 potassium channels at higher levels than in non-AD brains, and (2) Kv1.3 channels regulate Aβ-included microglial activation and effector functions *in-vitro*. In a blinded post-mortem immunohistochemical semi-quantitative analysis performed on ten Alzheimer's disease patients and 10 non-disease controls, we observed a significantly higher Kv1.3 staining intensity ($p=0.03$) and Kv1.3-positive cell density ($p=0.03$) in the frontal cortex of AD brains, compared to controls. This paralleled an increased number of Iba1-positive microglia in AD brains. We further confirmed increased Kv1.3 expression in AD brain by an objective and quantitative image analysis approach in hippocampal cortical sections from an independent sample of 5 AD and 5 non-AD cases. Increased Kv1.3 expression was also confirmed by western blot analysis of AD brain samples. Kv1.3-positive cells had microglial morphology and were associated with amyloid-β plaques. In immunofluorescence studies, Kv1.3 channels co-localized with Iba1 but not with astrocyte marker GFAP, confirming that elevated Kv1.3 expression in AD is limited to microglia. Consistent with our hypotheses, Aβ-induced reactive oxygen species productions as well as Aβ-induced impairment of microglial chemotaxis were inhibited by Kv1.3 channel blockade *in-vitro*. Our results demonstrate that Kv1.3 channels are highly expressed by microglia in human AD and also confirm that Kv1.3 channel blockade represents a promising strategy to inhibit pro-inflammatory microglial functions in AD.

Expression and functional importance of microglial Kv1.3 channels in Alzheimer's Disease

By

SRIKANT RANGARAJU

M.B.B.S., Tamil Nadu MGR University, India, 2007

Advisor: ALLAN I. LEVEY, MD, Ph.D.

A thesis submitted to the Faculty of the
James T. Laney School of Graduate Studies of Emory University

in partial fulfillment of the requirements for the degree of
Master of Science in Clinical Research

2016

Acknowledgements

The candidate would like to thank the advisor Dr. Allan I. Levey, the thesis committee members Dr. Amita Manatunga and Dr. Amit Shah for their guidance and mentorship, as well as collaborators Dr. Malu Tansey and Dr. Marla Gearing for their guidance and support.

The candidate would also like to acknowledge research funding support from the American Brain Foundation/American Academy of Neurology Clinical Research Training Fellowship in the Neurological Application of Neurotoxins (2014-2016), the Atlanta Clinical and Translational Science Institute, the Alzheimer's Disease Research Center for pilot funding and core facility support and the Emory Courtesy Scholarship Program.

Table of Contents

A. INTRODUCTION

AD is the most common dementing illness world-wide that results in disability, dependence and enormous health-care expenditure (1). Despite major advances in our understanding of disease mechanisms and pathogenesis, we currently do not have any treatments that modify the course of this devastating neurologic disease. The neuropathological hallmarks of AD include accumulation of Aβ plaques and neurofibrillary tangles as well as neuronal loss and microglial activation (2-4). Soluble Aβ peptides released from neurons and glia following sequential cleavage by enzymes called β and γ secretases form oligomeric and insoluble fibrillary forms that form Aβ aggregates that form the core of Aβ plaques. The robust accumulation of Aβ in AD, and the ability of Aβ-accumulating mouse models to recapitulate AD pathology and neurobehavioral deficits, supports the amyloid hypothesis of AD pathogenesis. In this model, Aβ accumulation exceeds the ability of Aβ clearing mechanisms in the brain, leading to neurodegeneration and cognitive deficits (5).

Aβ peptides (oligomeric and fibrillary forms) mediate neurotoxicity through direct mechanisms as well as indirectly through activation of immune cells in the brain called microglia (6, 7). Resting microglia normally remove Aβ peptides through phagocytosis while activated microglia that mediate pro-inflammatory functions have impaired abilities to clear Aβ peptides. Pro-inflammatory microglia release a variety of neurotoxic factors (cytokines such as interferon γ and tumor necrosis factor α, reactive oxygen species and nitric oxide). Aβ-induced microglial activation in AD precedes the clinical diagnosis of AD by many years. Recently, microglia gene mutations and polymorphisms have been found to significantly increase the risk of neurodegenerative diseases including AD. These results suggest that neuroinflammatory mechanisms mediated by microglia can modify the course of AD progression.(8) Understanding the key regulators of pro-inflammatory and neurotoxic microglial functions in AD may also lead

to the development of therapeutic approaches that selectively inhibit neurotoxic microglial functions while sparing neuroprotective functions.

Microglial functions, including neurotoxic effector functions described above, involve calcium influx into the cytoplasm. Sustained calcium entry into the cytoplasm is critical for immune cell function and requires potassium (K) ion extrusion from the cell in order to maintain the electrochemical gradient needed to maintain sustained calcium influx. These K extrusion pathways include potassium channels expressed on the microglial cell membrane. Resting microglia express very limited numbers of K channels, however upon activation by inflammatory stimuli (lipopolysaccharide or LPS), upregulate the voltage-gated K channel Kv1.3 in a highly selective manner. Therefore, calcium signaling in microglia activated by inflammatory stimuli is a Kv1.3 channel dependent process. Like LPS, Aβ peptides also induce microglial activation and upregulate Kv1.3 channel expression in *in-vitro* experiments (9).

Based on the existing body of literature on the disease-promoting and neurotoxic roles of pro-inflammatory activated microglia in AD pathogenesis and on experimental observations that Kv1.3 channels are upregulated by LPS and Aβ activated microglia, it is possible that microglial activation in AD is characterized by increased Kv1.3 channel expression and that pro-inflammatory microglial effector functions are dependent on Kv1.3 channel functions (10-13). Therefore, we propose two main hypotheses: (1) Activated microglia in human AD brains express Kv1.3 potassium channels at higher levels than in non-AD control brains, and (2) Kv1.3 channels regulate Aβ-included microglial activation and effector functions *in-vitro.*

B. BACKGROUND

Microglia mediate neuroinflammation in AD. Microglia represent the innate immunity of the central nervous system (CNS) and like macrophages, perform pro-inflammatory as well as regulatory functions (4, 14, 15). Classically activated M1 microglia induced by T cell cytokines tumor necrosis factor α and interferon γ are pro-inflammatory while M2 microglia have regulatory and anti-inflammatory functions (16). In AD, microglia surround amyloid plaques and contribute to amyloid turnover. It is suggested that early microglial activation in AD has a neuroprotective effect by promoting clearance of amyloid β (Aβ), however, in the later stages pro-inflammatory cytokines produced by activated microglia have detrimental effects that promote neurodegeneration (17). A central role for microglia in AD pathogenesis is supported by results from human genetic studies that confirmed an association between risk of AD and variations/polymorphisms in genes that encode microglial proteins. A mutation in triggering receptor expressed on myeloid cells 2 (TREM2), a microglial anti-inflammatory protein that represses microglial cytokine production and neuronal damage (18) confers an increased risk for late-onset AD (19). Increased expression of microglial protein CD33 is also associated with increased amyloid burden and single nucleotide polymorphisms in CD33 confer an increased risk for AD (20, 21). These results are congruent with data from animal models and support targeting of microglia in AD as a therapeutic strategy (22). However, non-selective genetic depletion of microglia does not alter neuropathological features in a mouse model of AD suggesting that anti-microglial strategies should target neurotoxic microglia, while sparing neuroprotective subsets (23). In addition, an understanding of cellular markers and pathways that define these microglial populations is critical in identifying novel therapeutic targets in AD (15, 22, 24).

Potassium channels are regulators of immune cell function and are novel therapeutic targets for human autoimmune disease. In immune cells such as lymphocytes, voltage-gated cation channels have been found to regulate cellular functions limited to distinct cell subsets that mediate autoimmunity, a finding of therapeutic relevance in human disease (25, 26). Voltage-gated potassium channels are key regulators of excitability in neurons and cardiac muscles; and of membrane potential in non-excitable tissues such as lymphocytes, platelets, macrophages and microglia (12, 25). Following membrane depolarization, efflux of potassium ions through open potassium channels in lymphocytes restores the electrophysiological gradient necessary to maintain calcium influx. Down-stream events following calcium entry drive cell migration, proliferation, activation and cytokine production. Human T cells primarily express Kv1.3 and KCa3.1 channels which regulate calcium entry (25). Upon activation, the majority of T cells up-regulate KCa3.1 channels while auto-reactive effector memory T cells preferentially up-regulate Kv1.3 channels, making them susceptible to Kv1.3-specific blockers (27). Kv1.3 channel-specific peptide toxins (ShK and its analogs [ShK-186, ShK-170, ShK-192] and PAP-1) as well as less selective Kv1 channel blockers (BgK and margatoxin) inhibit T cell proliferation, cytokine release and migration and can effectively ameliorate disease in animal models of autoimmunity (experimental allergic encephalomyelitis, pristane-induced arthritis and delayed-type hypersensitivity) without the side effects of non-specific immunosuppression (27). Potassium channels (Kv1.3, Kv1.5 and KCa3.1) are also expressed by microglia and macrophages (12, 28-30).

Kv1.3 potassium channels regulate membrane potential, calcium signaling and effector functions of activated microglia. Microglia are the key inflammatory cells in AD that mediate neuroinflammation and Kv1.3 channels are key regulators of microglial function. Microglial priming by Aβ in animal models of AD depends on a voltage-gated potassium channel Kv1.3 (31). Resting microglia express Kv1.5 channels and upon activation and proliferation, up-regulate

Kv1.3 and down-regulate Kv1.5 channels (31). Kv1.3 channels also migrate to the cell surface while Kv1.5 channels are internalized making Kv1.3 channels not only functionally relevant but also most susceptible to blockade by highly selective channel blockers (31). Microglial potassium channels also demonstrate a pattern of regulation that mirrors the pattern seen in human T lymphocytes (28, 29). Resting microglia express Kv1.5 channels, and upon activation by lipopolysaccharide, GM-CSF or interferon-γ, up-regulate Kv1.3 expression (12). Kv1.3 channels also control microglial proliferation, oxidative burst and neuronal killing (31-33). Small conductance calcium-activated potassium channel KCa3.1 is also expressed in microglia and blockade of this channel abrogates Aβ-induced neurotoxicity in murine models of AD (34, 35). TRPV1 channels seem to be of importance during Aβ-induced microglial activation and reactive oxygen species production. Inhibition of TRPV1 by 5-iodo-resiniferatoxin (RTX) abrogates ROS production by microglia (30). However, the "priming" of microglia by Aβ oligomers depends on Kv1.3 channels and is susceptible to inhibition by charybdotoxin and margatoxin but not RTX (9). Selective regulation of Kv1.3 channel expression by neuroinflammatory cytokines in AD could also alter microglial properties. Transforming growth factor-β (TGF-β) is a cytokine overexpressed by neurons in AD and is the only cytokine that is elevated in the cerebrospinal fluid of AD patients (36) and interestingly, treatment of microglia for 24 hours was found to increase microglial Kv1.3 channel expression in up to six-fold (37). The mechanisms underlying microglial polarity (pro-inflammatory M1 or anti-inflammatory or neuroprotective M2) are being defined and it is possible that altered expression of potassium channels could characterize these microglial states (22, 38). *In-vitro* data strongly support a role for Kv1.3 channels in Aβ-induced microglial dysfunction (9) but prior to this study, data demonstrating Kv1.3 expression in human AD brain tissue was lacking.

Kv1.3 channel blockade and deletion of Kv1.3 channels in animal models of human disease do not result in immunosuppression or neurologic sequelae. Selective brain-penetrating Kv1.3

channel blockers could target activated microglia while sparing other glial subtypes and neurons that do not express Kv1.3 channels at significant levels. Neurons express a wide variety of outward-rectifying potassium channels that predominantly include Kv1.2, 1.4, 1.6, 2.1 and small-conductance potassium (SK) channels, none of which are affected by the highly selective Kv1.3 channel blockers (ShK-186, Shk-170 and PAP-1) (39, 40). Kv1.3 channels are expressed in the olfactory bulb and a "super-smeller" phenotype in Kv1.3 -/- mice has been observed, but their expression in other cortical brain regions in low (41, 42). An FDA-approved non-specific blocker of Kv channel blocker, 4-aminopyridine, also blocks Kv1.3 channels and has a good safety profile in humans except for seizures at high doses (43, 44) that likely result from lowered seizure-threshold due to neuronal potassium channel blockade. In animal studies, treatment with ShK-186 and a CNS-penetrating Kv1.3 blocker PAP-1 did not increase their susceptibility to influenza and chlamydial infection (27, 45, 46). A human Phase 2A study of ShK-186 as a novel treatment for autoimmune diseases has also been completed with no observed adverse effects (47).

C. METHODS

Hypotheses:

(1) Activated microglia in human AD brains express Kv1.3 potassium channels at higher levels than in non-AD control brains, and

(2) Kv1.3 channels regulate Aβ-included microglial activation and effector functions *in-vitro.*

Research goals: This thesis dissertation has two main aims:

Aim 1: To compare Kv1.3 potassium channel protein expression in AD and non-AD post-mortem cortical brain tissue.

Aim 2: To test the *in-vitro* effect of Kv1.3 channel blockade with ShK-223 on (2A) Amyloid-β-induced reactive oxygen species (ROS) production, and (2B) Amyloid-β-induced inhibition of gap closure by BV2 microglia.

Study design:

Aim 1:

The first section was an observational cross-sectional neuropathological study of human post-mortem brain samples obtained from AD and non-AD control brains. Here, we compared levels of Kv1.3 channel protein expression between in AD and non-AD brains (frontal and hippocampal cortex) using immunohistochemistry and by Western-Blot analysis. We also described patterns of Kv1.3 channel protein expression based on specific cell types (microglia, astrocytes or neurons) that express Kv1.3 protein (using co-localization analysis) as well as detection of Kv1.3 expression in the vicinity of Aβ plaques (using double label immunohistochemistry).

Aim 2:

In the second section of this dissertation, we performed *in-vitro* experimental studies using the BV2 mouse microglial cell line as a model system to test the effects of Kv1.3 channel blockade (by ShK-223) on Aβ-induced microglial ROS production and on LPS and Aβ-induced inhibition of chemotaxis using the gap closure assay.

Aim 1: Study Population:

Definition of AD Case: Post-mortem brain tissue (frontal cortex) from a patient pathologically confirmed to have AD only, collected within 12 hours post-mortem interval (PMI). Definition of *Non-AD Control:* Post-mortem brain tissue (frontal cortex) from patient with no evidence of neurodegenerative disease based on pathology and no clinical signs of cognitive impairment.

Matching: Age matching (+/- 5 years) and Gender Matching. Blinding: Both raters were blinded to diagnosis at time of immunostaining as well as grading. Un-blinding was performed after collection and tabulation of data. Pathologic grading was performed by both raters independently.
Brain tissues: Ten AD brains and 10 age-matched non-disease control cryopreserved brain tissues were randomly selected from a neuropathologic repository from the Emory Alzheimer Disease Research Center Neuropathology Core, Atlanta. 12 µm sections from paraffin-embedded frontal cortical brain tissue were prepared. The samples were alphanumerically coded prior to blinded immunohistochemical analysis.
Sample characteristics: Patient's age at death, sex and race (Caucasian vs. non-Caucasian), ApoE allelic status (2/3, 3/3, 3/4, 4/4) and Braak neuropathological grade (0-VI) and post-mortem interval (hours) were collected for each sample (48). The Braak neuropathological grade is a 7 point scale that indicates extent of amyloid plaques and neurofibrillary tangles detected in the brain. A score of 0 indicates no AD pathology while a score of VI indicates very extensive pathology involving all brain regions. Normal ageing is frequently associated with Braak stages of 0-II during brain autopsy in the absence of any cognitive decline (49).

Aim 1: Analytic approach and statistical considerations:

The primary outcomes of this Aim are median Kv1.3 staining intensity and median Kv1.3 staining density. Covariate that was assessed was disease status (AD vs. non-AD status). Our Null Hypothesis was that median Immunostaining intensity and median immunostaining density of Kv1.3 channel protein in the frontal cortex of AD and non-AD control post-mortem brain specimens are equal. Our alternative hypothesis was that median Immunostaining intensity and median immunostaining density of Kv1.3 channel protein in AD frontal cortex is not equal that of non-AD control post-mortem frontal cortex brain specimens. We used the non-parametric Mann-Whitney U test for comparisons between groups At α level 0.05, power 0.80 and expected difference in median staining intensity of 1.0 unit and SD of sample population 0.75, we required at least n=9 per group in the study. We proceeded with 10 AD and 10 non-AD controls (power=0.85, α=0.05). *Inter-rater agreement was also assessed.* Mean staining intensity and staining density for each sample by each rater was used for calculation of intra-class correlation coefficient (50).

Aim 1: Research methods:

Antibodies: Rabbit anti-human Kv1.3 polyclonal IgG (Catalog # APC101) was obtained from Alomone Laboratories, Jerusalem. Optimization for immunohistochemistry on paraffin embedded tissue was performed on control brain tissue as well as mouse spleen tissue (positive control) and dilution of 1:100 was selected. Goat anti-Iba1 polyclonal Ab (Abcam #ab5076) was used at 1:200 dilution. Appropriate goat anti-rabbit (Sigma-Aldrich, 1:1000) and horse anti-goat IgG (Sigma, 1:1000) were used as secondary antibodies. Anti-GFAP mAb (Millipore MB360) was used to label astrocytes and Anti-Aβ monoclonal 4G8 (Aβ 17-24) antibody (Covance SIG 39245) was used to identify amyloid plaques.

Immunohistochemistry on paraffin sections: Paraffin-embedded sections were deparaffinized through an alcohol gradient, heated in a microwave in 10 mM citric acid (pH 6.0) for 15 min,

blocked with 0.3% hydrogen peroxide for 30 minutes and then blocked with 4% normal goat serum/0.4% Triton X-100/Tris-buffered saline (TBS) for 1 h, followed by overnight incubation with primary anti-Kv1.3 antibody or anti-Iba1 antibody. Sections were rinsed with TBS and incubated with appropriate biotin-conjugated secondary antibody followed by Vectastain Elite ABC and diaminobenzidine (DAB) as per manufacturer's recommendations. To exclude nonspecific staining unrelated to polyclonal and monoclonal antibodies, immunostaining was performed with omission of the antibodies but with all other procedures unchanged in some experiments. Slides were lastly counterstained with hematoxylin. Specificity of anti-Kv1.3 antibody was determined in two AD samples by pre-adsorption with Kv1.3 peptide (8 µg/ml, Alomone laboratories) followed by further immunostaining with primary and secondary antibodies as described above. For double antigen immunohistochemistry for Kv1.3 and Aβ, slides were first immunostained with anti-Kv1.3 Ab, secondary Ab and developed with Vectastain Elite ABC and DAB chromogen. This was followed by antigen retrieval with 98% formic acid and incubation with anti-Aβ antibody (4G8, 1:2000) for 1 hour. Secondary Ab incubation was followed by Vectastain Elite ABC and SG-Blue chromogen per manufacturer's protocol. Light microscopy was performed with an Olympus light microscope (Olympus, Center Valley, PA).

Pathologic grading: Ten AD cases and 10 control specimens that were immunostained for Kv1.3 and Iba1 were independently evaluated by two blinded investigators. Staining intensity of positive cells at 20x magnification, based on intensity of DAB labelling, was graded as follows: 0 – no staining, 1 – mild, 2- moderate, 3 – strong. Examples of each grade were provided to each observer for reference. Staining density, defined as number of positive cells per 20x power field, was graded as follows: 0 – no positive cells/field, 1 – 1-10/field, 2 – 11-50/field, 3 - ≥ 50/field. Each observer rated 3 cortical fields and 3 white matter fields per slide for staining intensity and

density and the mean score was used as a final grade. Inter-observer agreement was calculated. Median staining intensity and staining density was compared between AD cases and controls.

Objective image analysis of immunohistochemistry data using ImageJ software: In an independent sample of 5 AD and 5 non-AD hippocampal cortical post-mortem brain tissue, matched for Age (±5 years) and Sex, we performed immunostaining for Kv1.3 (brown staining) and nuclei (blue/Hematoxylin) in a blinded manner. At 10x magnification, we captured 3 cortical regions from each patient sample. Each acquired image was processed using ImageJ software using an additional plugin for deconvolution that separated brown staining from blue staining. All non-specific background brown staining was subtracted using data from control sections stained without the primary anti-Kv1.3 antibody. Then, brown staining was converted to gray scale and the number of pixels with brown (Kv1.3) staining in each section were quantified using an automated algorithm. The average Kv1.3 positivity for each sample was used for final analysis. See Fig. x for further details regarding this approach. Un-blinding was performed followed by grouping of data into AD and non-AD cases, followed by statistical analysis. For this sub-study that did not have a pre-specified power calculation, we used the Mann-Whitney U test for non-parametric comparison (alpha level 0.05).

Immunofluorescence microscopy and co-localization analysis: Slides from 3 AD cases and 3 controls were incubated with rabbit anti-Kv1.3 (1:100) and goat anti-Iba1 (1:200) or rabbit anti-Kv1.3 and mouse anti-GFAP mAb (1:500) antibodies. Phycoerythrin-conjugated Donkey anti-rabbit IgG (1:1000), Fluorescein Isothiocyanate (FITC)-conjugated donkey anti-goat and FITC-conjugated goat anti-mouse IgG (1:1000) were used as secondary antibodies. Pre-incubation of tissue with 10% cupric sulfate was used to minimize background staining due to lipofuschin. Single antibody controls for each channel were used to optimize settings for image acquisition. Nonspecific staining was evaluated by omission of primary antibodies but with all other steps. Images were acquired at 20x and 40x magnification on an Olympus microscope. Three

representative images in each group at 20x magnification were picked for co-localization analysis using ImageJ software (51). Degree of co-localization was defined as the percentage of pixels positive on both channels, expressed over a denominator of all pixels that were positive on either channel. Thresholds for positivity were defined based on control slides where primary antibody was omitted. Average degree of co-localization (n=3 images/case, N=3 per group) in AD cases and controls were compared using Student's t-test ($p \leq 0.05$ was considered significant for a two-tailed analysis). For co-localization experiments using immunofluorescence microscopy, appropriate FITC-conjugated antibodies for anti-Iba1 primary or anti-GFAP primary and PE-conjugated anti-rabbit secondary antibodies were used. After nuclear staining with 4′,6′-diamidino-2-phenylindole (DAPI) for 10 min, sections were cover-slipped with glycerol, and fluorescent images were obtained with a fluorescence microscope (Olympus) using FITC, PE and DAPI filters and images were processed using Zeiss LSM Image Browser.

Western-Blot analyses: We used 4 AD and 5 non-AD frontal cortex whole brain homogenates for immunoblotting experiments. Briefly, 8M urea lysates of 250 mg of brain tissue from each sample were prepared after extensive sonication and homogenization. The homogenates were centrifuged at 15000g for 30 minutes and the supernatants were used for further testing. Protein concentrations were measured using the Bradford assay to estimate total protein concentrations per sample. Equal amounts of protein (25µg) were loaded in each lane of 10 lane SDS polyacrylamide electrophoresis gels. After transfer of protein to nitrocellulose membranes, Kv1.3 antibody (1:1000 dilution) was added for 24 hour incubation (4 degrees C), followed by secondary amplification with appropriate secondary antibodies. Simultaneously, Na/K ATPase protein was also measured as a reference standard for each sample. The intensity of the Kv1.3 band detected was measured by optical densitometry. Non-normalized and normalized densitometric data were used for comparison across AD and non-AD groups using a independent sample 2-tailed T test assuming equal variance (α level 0.05).

Aim 2: Study design, analytical plan and statistical considerations:

(2A) In-vitro assays of microglial ROS production:

Assay: The cell permeant reagent 2',7' –dichlorofluorescin diacetate (DCFDA) is a fluorogenic dye that measures hydroxyl, peroxyl and other reactive oxygen species (ROS) activity within the cell. After diffusion in to the cell, DCFDA is deacetylated by cellular esterases to a non-fluorescent compound, which is later oxidized by ROS into 2', 7' –dichlorofluorescein (DCF). DCF is a highly fluorescent compound which can be detected by fluorescence spectroscopy with maximum excitation and emission spectra of 495 nm and 529 nm respectively. Microglia were loaded with DCFDA for 30 minutes followed by washing three times, and then incubated with Aβ42 fibrils (1μM final concentration) for 1 hour with or without Kv1.3 blocker ShK-223 (10 nM final concentration). Appropriate DCFDA-only, blank and ShK-223 only controls were performed in parallel. After 1 hour, ROS production was measured by detection of green fluorescence using a fluorescence plate reader. Each condition was performed 5 times. One-way ANOVA was performed to detect overall differences in ROS production across all treatment groups. Independent sample 2-tailed T test were performed for pairwise comparisons, assuming equal variance.

The primary outcome of this experiment was Aβ42-induced mean ROS production at 1 hour and the covariate was Kv1.3 blocker (ShK-223) versus vehicle treatment. Our null hypothesis was that mean ROS production in "Aβ" and "Aβ+ShK-223" treated groups are the same. Our alternative hypothesis was that mean ROS production in "Aβ" and "Aβ+ShK-223" treated groups are different. The *treatment conditions were* (1) DCFDA-only control, (2) DCFDA + ShK-223, (3) DCFDA + Aβ42, DCFDA + (4) Aβ42 + ShK with n=5 replicates for each condition. Using the one-way ANOVA test to compare mean ROS production across treatment groups at power=0.80 and α=0.01 to detect a difference of at least 200 ROS units between two groups and 5 post-hoc pairwise t-tests, we needed n=5 samples per group.

(2B) In-vitro assays of microglia chemotaxis (gap closure assay):

Assay: The gap closure assay is an assay of chemotaxis in-vitro in response to local tissue damage. Following placement of a scratch/gap in near confluent cells, the normal response is that the surrounding cells migrate and fill the gap within 18-24 hours. Activating stimuli such as lipopolysaccharide (LPS) impair the ability of microglia to close the gap. In our experiment, BV2 cells were grown to near confluence in the absence of serum in the culture medium. Aβ42 (1μM) or LPS (100 ng/mL) were then added to the culture medium following which a uniform scratch was placed in the plate at two locations using a 200 microliter micropipette tip. The width of the gap was measured in 6 locations for each scratch. After 24 hours, the scratch width was measured again at 6 locations. Two gaps were placed in each culture dish and each condition had 5 biological replicates. The effect of ShK-223 alone and in the presence of Aβ42 was tested and appropriate negative controls were performed. Percentage gap closure was (using the time 0 reading as baseline) was measured for each gap in each condition and group wise comparisons of mean gap closure were performed.

The primary outcome for these experiments were mean % gap closure at 24 hours and the covariate was Kv1.3 blocker (ShK-223) versus vehicle treatment. Our null hypothesis was *that* ShK-223 does not affect amyloid-β/LPS induced inhibition of microglial gap closure. Our alternate hypothesis was that ShK-223 reduces amyloid-β/LPS-induced inhibition of microglial gap closure. The treatment conditions were as follows: Experiment 1: Control, ShK-223 only, LPS only, LPS + ShK-223. N=5 replicates per condition; (2) Experiment 2: Control, ShK-223 only, Aβ42 only, Aβ42 + ShK-223. N=5 replicates per condition. Using the one-way ANOVA test to compare mean % gap closure across treatment groups at power=0.80 and α=0.01, to detect a difference of at least 25% in gap closure between two groups and 5 post-hoc pairwise t-tests, we needed at least 5 samples per group.

D. RESULTS

D 1. AIM 1. To compare Kv1.3 potassium channel protein expression in AD and non-AD post-mortem cortical brain tissue.

Patient characteristics. Baseline characteristics of the study population used for Aim 1 are presented in Table 1. The AD and non-AD groups had comparable age, sex and race distributions. Mean post-mortem intervals were also similar in both groups (AD 9.3±6.5 hours, non-AD 8.6±3.3 hours). As expected, AD cases had a higher Braak neuropathological grade as compared to non-AD controls (Braak stage III-VI seen in 100% AD cases vs. 0% in non-AD controls, Fisher exact $p<0.001$). Similarly, ApoE 4 allelic status was also more frequent among AD cases as compared to non-AD controls (Fisher exact $p=0.011$).

Acceptable inter-rater agreement between two observers recording Kv1.3 staining intensity and staining density. Frontal lobe paraffin-embedded tissue from 10 AD cases and 10 control cases were stained individually for Kv1.3 and microglial marker Iba1 and graded in a blinded manner as described above. There was acceptable agreement between the two raters (intra-class coefficient 0.68 for staining density and 0.73 for staining intensity).

Kv1.3 channel protein expression and microglial Iba1 marker expression are increased in frontal and hippocampal cortex of human post-mortem AD brains as compared to non-AD controls. In a combined analysis from both raters, cortical regions of AD brains showed higher density ($p=0.002$) of $Iba1^{positive}$ microglia (Table 2, Figure 2) suggesting increased microglial proliferation in AD. Cortical regions of AD brains had higher Kv1.3 staining intensity ($p=0.03$) and higher density ($p=0.03$) of $Kv1.3^{positive}$ cells. In an independent experiment with 5 AD and 5 non-AD cases using an objective image analysis based approach to quantify Kv1.3 staining in AD, we found that median immunostaining positivity for Kv1.3 channel protein was significantly higher in the hippocampal cortex of AD cases compared to non-AD controls (Figure 3, Mann-

Whitney U test p=0.003). Surprisingly, we also found a significantly increased Kv1.3 staining pattern in Parkinson's disease patients as compared to non-AD/non-PD controls (Mann-Whitney U test p=0.027). In Western-Blot analyses of 4 AD and 5 non-AD frontal cortical brain samples, we also confirmed that Kv1.3 channel protein expression is significantly higher in AD brains compared to non-AD samples (Figure 4).

Kv1.3 expression in the AD brain is restricted to microglia and not astrocytes or neurons. In order to confirm the cellular localization of Kv1.3 in AD brain tissue, we performed immunofluorescence microscopy using antibodies directed against microglia (Iba1, anti-goat polyclonal IgG, 1:200), astrocytes (GFAP, mouse monoclonal IgG, 1:500) and Kv1.3 channels (goat anti-rabbit polyclonal, 1:100). Degree of co-localization between Kv1.3 and Iba1 was significantly higher than that between Kv1.3 and GFAP (Figure 5). No co-localization between Kv1.3 and neuronal marker (Tuj1) was observed. These results confirm that Kv1.3 channels are primarily expressed by microglia in human AD brains.

Kv1.3 channels and Iba1^{positive} microglia are found in the vicinity of amyloid plaques in AD. If increased Kv1.3 channel expression is related to AD pathogenesis, these channels should be expressed by glia in close proximity to amyloid plaques, the hallmark of AD. In dual-chromogen immunohistochemistry experiments simultaneously probing for Kv1.3 and Aβ, we observed that Kv1.3^{positive} cells predominated in the vicinity of amyloid plaques (Figure 6, n=3 AD cases) in AD frontal cortex.

Anti-Kv1.3 antibody detects Kv1.3 channel protein with high specificity. In an experiment to confirm the specificity of the anti-Kv1.3 antibody used in this study, we pre-adsorbed the anti-Kv1.3 antibody with saturating amounts of the immunogenic peptide before performing immunohistochemistry. Peptide pre-adsorption abolished all Kv1.3 staining in AD brains confirming the specificity of this antibody (Figure 7).

D 2. AIM 2. To test the *in-vitro* effect of Kv1.3 channel blockade with ShK-223 on (2A) Amyloid-β-induced reactive oxygen species (ROS) production, and (2B) Amyloid-β-induced inhibition of gap closure by BV2 microglia.

Kv1.3 channel blockade by ShK-223 inhibits Aβ42 fibril-induced ROS production by BV2 microglia. Median ROS production levels were significantly different across the treatment groups in our experiment (Figure 8, One-way ANOVA p value <0.001, F statistic 1929, df=3). As compared to the DCFDA control condition, ShK-223 (10 nM) resulted in a significant, although small reduction in ROS production suggesting a possible anti-oxidant effect of ShK-223. Aβ42 treatment resulted in a statistically significant 2-fold increase in ROS production ($p<0.0001$ as compared to DCFDA control) at 1μM concentrations, but not at lower concentrations. This effect was completely reversed by combined treatment of ShK-223 ($p<0.0001$ comparing Aβ42+ShK-223 and Aβ42 groups). Since the DCFDA fluorescence quenches over 1-2 hours, longer experiments could not be performed with lower concentrations. In 1 hour experiments, there was no visible cell death seen in Aβ42-treated BV2 cells.

LPS-mediated and Aβ42-mediated inhibition of microglial gap closure is partly reversed by Kv1.3 channel blockade by ShK-223. In gap closure assays of BV2 microglia using two experimental paradigms (LPS or Aβ42-induced gap closure inhibition), significant differences in mean percentage of gap closure were seen across treatment groups (Figure 9, one-way ANOVA p values <0.001 for both experiments, Figures 9B and C). In the LPS experiment (Figure 9B), LPS at 100 ng/mL inhibited gap closure by 53% ($p<0.001$ comparing Control and LPS-treated groups). ShK-223 treatment alone had no effect on gap closure confirming absence of direct toxicity of the Kv1.3 channel blocker ($p>0.05$). ShK-223 treatment, however, partly reversed the effect of LPS on gap closure inhibition ($p<0.01$ for T-test comparing LPS+ShK-223 to LPS-alone treatment groups). Similar results were obtained in experiments where Aβ42 (Figure 9C) was

used as an *in-vitro* stimulus for microglia. Aβ42 treatment completely inhibited gap closure by BV2 microglia at 0.1μM concentrations ($p<0.001$ comparing Control and Aβ42-alone treatment groups). ShK-223 treatment partly reversed the Aβ42 effect ($p=0.01$ comparing Aβ42+ShK-223 to Aβ42-alone treatment groups). However, roughly 50% of the Aβ42 effect was not reversed by ShK-223, suggesting a partial effect. At higher doses of Aβ42 (1μM), we observed direct toxicity resulting in BV2 cell death at 24 hours. As a result, effect of ShK-223 at higher Aβ42 concentrations could not be assessed in the gap closure assay.

E. DISCUSSION

The microglial potassium channel Kv1.3 is a known regulator of microglial activation and effector functions but its relevance to neurodegenerative diseases such as AD, is currently unknown (11, 13, 52). Using a combination of neuropathological and *in-vitro* experimental approaches, we show that (1) Kv1.3 channel protein in expressed at higher levels in the AD brain as compared to non-AD control brains in both frontal and hippocampal cortical regions, as evidenced by immunohistochemistry as well as by Western Blot analyses; (2) Kv1.3 expression in the AD brain is restricted primarily to microglia in the frontal cortical regions and to microglia that are in the vicinity of Aβ plaques; (3) Aβ-induced ROS production by BV2 microglia can be inhibited by Kv1.3 channel blockade by ShK-223; and (4) Inhibition of microglial chemotaxis induced by LPS and Aβ fibril treatment are both partly reversed by Kv1.3 channel blockade by ShK-223.

Our data represents the first demonstration of increased Kv1.3 channel expression in a human neurodegenerative disease. Prior work by others has shown that activated microglia upregulate Kv1.3 channels and LPS-induced microglial effector functions can be inhibited by Kv1.3 channel blockade (9, 31, 33). A nearly two fold increase in levels of Kv1.3 channel gene expression has also been observed in microglia isolated from the 5xFAD transgenic mouse model of AD that rapidly accumulates Aβ plaque pathology (53, 54). Based on our results, it is likely that the assessment of microglial Kv1.3 channel expression and the effects of Kv1.3 channel blockade in rodent models AD are also likely to apply to human disease.

We also found that Kv1.3 channels are expressed in the non-AD brain at a low level and in a non-neuronal distribution. This observation is important because microglial Kv1.3 expression can be therapeutically relevant only if the channel is not expressed diffusely by normal neurons and glia. Selective blood brain barrier-penetrating Kv1.3 channel blockers could target activated

microglia while sparing other glial subtypes and neurons that do not express Kv1.3 channels at significant levels. Neurons express a wide variety of outward-rectifying potassium channels that predominantly include Kv1.2, 1.4, 1.6, 2.1 and small-conductance potassium (SK) channels, none of which are affected by the highly selective Kv1.3 channel blockers (ShK-186, Shk-170 and PAP-1) (39, 40). Kv1.3 channels are expressed in the olfactory bulb and a "super-smeller" phenotype in Kv1.3 -/- mice has been observed, but their expression in other cortical brain regions in low (41, 42). An FDA-approved non-specific blocker of Kv channels, 4-aminopyridine, also blocks Kv1.3 channels and has a good safety profile in humans except for seizures at high doses (43, 44) that likely result from lowered seizure-threshold due to neuronal potassium channel blockade. In animal studies, treatment with ShK-186 and a CNS-penetrating Kv1.3 blocker PAP-1 did not increase their susceptibility to influenza and chlamydial infection (27, 45, 46). Although the neurologic safety profile of selective Kv1.3 blockers in humans has not been demonstrated, the above observations suggest that selective Kv1.3 blockade may not result in significant neurologic or immunosuppressive adverse effects. A human Phase 2A study of ShK-186 as a novel treatment for autoimmune diseases has also been completed with no observed adverse effects (47). Kv1.3 channels expressed by pro-inflammatory microglia may represent therapeutic targets for neuro-immunomodulatory drugs for the treatment of AD.

The relevance of microglial Kv1.3 channels in neuroinflammation is also likely to extend beyond AD. For example, activated microglia after status epilepticus up-regulate a potassium channel electro-physiologically identical to Kv1.3 (55). HIV-Tat also induces Kv1.3 channel expression in microglia and blockade with 4-aminopyridine seems to abrogate neurotoxicity in-vitro (56). Altered Kv1.3 channel regulation in microglia and blood-derived dendritic cells has also been observed in neuroinflammatory disease states such radiation-induced brain injury and multiple sclerosis (29, 57). Although we showed that microglia that are classically activated by LPS and Aβ42 in an AD-relevant manner utilize Kv1.3 channels to mediate their neurotoxic

functions, we did not assess functional relevance of Kv1.3 or other K channels in anti-inflammatory or M2 microglia in AD. Others have found that genes downregulated by microglia upon LPS stimulation include non-Kv1.3 channels such as Kir2.1, KCa3.1 and purinergic cationic channels (P2X4 and P2X7). (13, 53, 54) These findings raise the possibility that microglia polarized towards the pro-inflammatory spectrum of activation have a distinct ion channel expression patterns while those polarized towards the anti-inflammatory or protective spectrum may utilize alternative ion channels to regulate calcium signaling and effector functions. We speculate that selective inhibition of pro-inflammatory neuroinflammatory responses in AD brain may be possible by targeting Kv1.3 channels while sparing and/or promoting protective functions. These possibilities will be explored in ongoing in-vivo studies in mouse models of AD pathology.

Strengths and limitations:

A major strength of this study is the combined use of neuropathological observational data and experimental *in-vitro* data to show the expression and functional relevance of Kv1.3 channels in AD. Our neuropathological studies were statistically well-powered. We also reproduced our main result in Aim 1 in two additional independent experimental approaches. We found increased Kv1.3 channel protein expression by semi-quantitative immunostaining using a staining intensity and density rating scale and also obtained the same result using a more objective a quantitative image-analysis based approach. We showed that the antibody we used for neuropathological and western blotting studies detected Kv1.3 channel protein with high specificity and low background staining or non-specific protein detection. Our *in-vitro* studies were also adequately powered to detect our pre-specified differences. We used a highly-selective blocker of Kv1.3 channels called ShK-223 in our experiments. ShK-223 blocks KV1.3 channels with over 10,000-fold higher

affinity than for other Kv channels. At 10 nM concentrations used in our studies, we expect at least 95% of Kv1.3 channels to be blocked by ShK-223 with no additional blockade of any other non-Kv1.3 channel. While immunohistochemistry detects all KV1.3 channel protein (cell surface and intracellular), our *in-vitro* assays tested the importance of only cell surface and functionally important Kv1.3 channels. These strengths allow us to confidently conclude that the observed effects of ShK-223 on Aβ42-induced microglial ROS production and effects on chemotaxis are a result of blockade of functionally relevant Kv1.3 channels.

Certain limitations of this study also need to be acknowledged. In Aim 1, we utilized only one anti-Kv1.3 polyclonal antibody for all the immunohistochemical studies. Although the antibody we used was highly specific for our channel of interest, other commercially available Kv1.3 antibodies were found to be non-specific with high background staining in our hands. We are currently validating a new anti-Kv1.3 antibody and plan to confirm our observations in a limited sample of AD and non-AD cases in the future using this new antibody, in order to further validate our results. The inter-rater reliability in the semi-quantitate part of Aim 1 was adequate (ICC 0.6-0.7) but was not high. This may have resulted in increased variability in median Kv1.3 staining intensity and density measures. To overcome this limitation, we performed a more objective and quantitative image analysis approach and confirmed our primary finding. Another limitation of immunohistochemistry was that it did not allow us to distinguish between intracellular and cell surface Kv1.3 channel proteins. Functionally relevant Kv1.3 channels are those that reside on the cell surface. Future studies using freshly frozen brain specimens (as opposed to paraffin embedded specimens) may overcome this limitation. In addition, we are currently performing whole-cell patch clamp on freshly isolated microglia from AD patients and non-AD patients to address this limitation.

In summary, we have demonstrated that Kv1.3 expression is increased in the frontal and hippocampal cortex of humans with AD as compared to non-AD controls. Kv1.3 channels are

abundantly expressed in the vicinity of Aβ plaques and are primarily expressed by microglia as demonstrated by co-localization between Kv1.3 and Iba1. Inhibition of Kv1.3 channels by highly selective peptide blocker ShK-223 inhibits Aβ42-induced ROS production as well as partly reversed Aβ42-induced inhibition of microglial chemotaxis *in-vitro*. In context of the growing body of literature suggesting a role for microglia in neurodegeneration, and for potassium channels in microglial physiology, our results provide evidence that microglial Kv1.3 channels represent therapeutic targets in human neuroinflammatory and neurodegenerative disorders such as AD. The translational potential of our findings are also very exciting because a Kv1.3 blocking ShK peptide (ShK-186) has recently successfully completed Phase 2A human clinical studies for systemic autoimmune diseases with satisfactory safety profiles. Future studies are now needed to investigate the therapeutic effect of Kv1.3 channel blockade on neuropathological, neurobehavioral and safety outcome measures in animal models of AD.

F. REFERENCES

1. Alzheimer's A. 2015 Alzheimer's disease facts and figures. *Alzheimer's & dementia : the journal of the Alzheimer's Association* 2015;11(3):332-84.
2. Mandrekar-Colucci S, Landreth GE. Microglia and inflammation in Alzheimer's disease. *CNS & neurological disorders drug targets* 2010;9(2):156-67.
3. Cameron B, Landreth GE. Inflammation, microglia, and Alzheimer's disease. *Neurobiology of disease* 2010;37(3):503-9.
4. Heppner FL, Ransohoff RM, Becher B. Immune attack: the role of inflammation in Alzheimer disease. *Nature reviews Neuroscience* 2015;16(6):358-72.
5. Karran E, Mercken M, De Strooper B. The amyloid cascade hypothesis for Alzheimer's disease: an appraisal for the development of therapeutics. *Nature reviews Drug discovery* 2011;10(9):698-712.
6. Iwatsubo T, Saido TC, Mann DM, et al. Full-length amyloid-beta (1-42(43)) and amino-terminally modified and truncated amyloid-beta 42(43) deposit in diffuse plaques. *The American journal of pathology* 1996;149(6):1823-30.
7. Sondag CM, Dhawan G, Combs CK. Beta amyloid oligomers and fibrils stimulate differential activation of primary microglia. *Journal of neuroinflammation* 2009;6:1.
8. Hensley K. Neuroinflammation in Alzheimer's disease: mechanisms, pathologic consequences, and potential for therapeutic manipulation. *Journal of Alzheimer's disease : JAD* 2010;21(1):1-14.
9. Schilling T, Eder C. Amyloid-beta-induced reactive oxygen species production and priming are differentially regulated by ion channels in microglia. *Journal of cellular physiology* 2011;226(12):3295-302.
10. Butovsky O, Jedrychowski MP, Moore CS, et al. Identification of a unique TGF-beta-dependent molecular and functional signature in microglia. *Nature neuroscience* 2014;17(1):131-43.
11. Charolidi N, Schilling T, Eder C. Microglial Kv1.3 Channels and P2Y12 Receptors Differentially Regulate Cytokine and Chemokine Release from Brain Slices of Young Adult and Aged Mice. *PloS one* 2015;10(5):e0128463.
12. Fischer HG, Eder C, Hadding U, et al. Cytokine-dependent K+ channel profile of microglia at immunologically defined functional states. *Neuroscience* 1995;64(1):183-91.
13. Lam D, Schlichter LC. Expression and contributions of the Kir2.1 inward-rectifier K(+) channel to proliferation, migration and chemotaxis of microglia in unstimulated and anti-inflammatory states. *Frontiers in cellular neuroscience* 2015;9:185.
14. Lehnardt S. Innate immunity and neuroinflammation in the CNS: the role of microglia in Toll-like receptor-mediated neuronal injury. *Glia* 2010;58(3):253-63.
15. Weitz TM, Town T. Microglia in Alzheimer's Disease: It's All About Context. *Int J Alzheimers Dis* 2012;2012:314185.
16. Varnum MM, Ikezu T. The classification of microglial activation phenotypes on neurodegeneration and regeneration in Alzheimer's disease brain. *Arch Immunol Ther Exp (Warsz)* 2012;60(4):251-66.
17. Hickman SE, Allison EK, El Khoury J. Microglial dysfunction and defective beta-amyloid clearance pathways in aging Alzheimer's disease mice. *J Neurosci* 2008;28(33):8354-60.
18. Jiang T, Yu JT, Zhu XC, et al. TREM2 in Alzheimer's disease. *Mol Neurobiol* 2013;48(1):180-5.
19. Jonsson T, Stefansson H, Steinberg S, et al. Variant of TREM2 associated with the risk of Alzheimer's disease. *N Engl J Med* 2013;368(2):107-16.

20. Griciuc A, Serrano-Pozo A, Parrado AR, et al. Alzheimer's disease risk gene CD33 inhibits microglial uptake of amyloid beta. *Neuron* 2013;78(4):631-43.
21. Bradshaw EM, Chibnik LB, Keenan BT, et al. CD33 Alzheimer's disease locus: altered monocyte function and amyloid biology. *Nature neuroscience* 2013;16(7):848-50.
22. Saijo K, Glass CK. Microglial cell origin and phenotypes in health and disease. *Nat Rev Immunol* 2011;11(11):775-87.
23. Colton CA. Heterogeneity of microglial activation in the innate immune response in the brain. *J Neuroimmune Pharmacol* 2009;4(4):399-418.
24. Grathwohl SA, Kalin RE, Bolmont T, et al. Formation and maintenance of Alzheimer's disease beta-amyloid plaques in the absence of microglia. *Nature neuroscience* 2009;12(11):1361-3.
25. Cahalan MD, Chandy KG. The functional network of ion channels in T lymphocytes. *Immunol Rev* 2009;231(1):59-87.
26. Rangaraju S, Chi V, Pennington MW, et al. Kv1.3 potassium channels as a therapeutic target in multiple sclerosis. *Expert Opin Ther Targets* 2009;13(8):909-24.
27. Beeton C, Wulff H, Standifer NE, et al. Kv1.3 channels are a therapeutic target for T cell-mediated autoimmune diseases. *Proc Natl Acad Sci U S A* 2006;103(46):17414-9.
28. Kaushal V, Koeberle PD, Wang Y, et al. The Ca2+-activated K+ channel KCNN4/KCa3.1 contributes to microglia activation and nitric oxide-dependent neurodegeneration. *J Neurosci* 2007;27(1):234-44.
29. Mullen KM, Rozycka M, Rus H, et al. Potassium channels Kv1.3 and Kv1.5 are expressed on blood-derived dendritic cells in the central nervous system. *Ann Neurol* 2006;60(1):118-27.
30. Schilling T, Eder C. Importance of the non-selective cation channel TRPV1 for microglial reactive oxygen species generation. *J Neuroimmunol* 2009;216(1-2):118-21.
31. Kotecha SA, Schlichter LC. A Kv1.5 to Kv1.3 switch in endogenous hippocampal microglia and a role in proliferation. *J Neurosci* 1999;19(24):10680-93.
32. Khanna R, Roy L, Zhu X, et al. K+ channels and the microglial respiratory burst. *Am J Physiol Cell Physiol* 2001;280(4):C796-806.
33. Fordyce CB, Jagasia R, Zhu X, et al. Microglia Kv1.3 channels contribute to their ability to kill neurons. *J Neurosci* 2005;25(31):7139-49.
34. Skaper SD. Ion channels on microglia: therapeutic targets for neuroprotection. *CNS & neurological disorders drug targets* 2011;10(1):44-56.
35. Maezawa I, Zimin PI, Wulff H, et al. Amyloid-beta protein oligomer at low nanomolar concentrations activates microglia and induces microglial neurotoxicity. *J Biol Chem* 2011;286(5):3693-706.
36. Swardfager W, Lanctot K, Rothenburg L, et al. A meta-analysis of cytokines in Alzheimer's disease. *Biol Psychiatry* 2010;68(10):930-41.
37. Schilling T, Quandt FN, Cherny VV, et al. Upregulation of Kv1.3 K(+) channels in microglia deactivated by TGF-beta. *Am J Physiol Cell Physiol* 2000;279(4):C1123-34.
38. Maezawa IJ, David; Sexton, Jessica; Wulff, Heike; Jin, Lee-Way The role of potassium channel Kv1.3 in Aß-induced microglia activation [abstract]. *Alzheimer's & Dementia* 2012;PII: S1552-5260(12)00949-1.
39. Gutman GA, Chandy KG, Adelman JP, et al. International Union of Pharmacology. XLI. Compendium of voltage-gated ion channels: potassium channels. *Pharmacol Rev* 2003;55(4):583-6.
40. Grissmer S, Nguyen AN, Aiyar J, et al. Pharmacological characterization of five cloned voltage-gated K+ channels, types Kv1.1, 1.2, 1.3, 1.5, and 3.1, stably expressed in mammalian cell lines. *Mol Pharmacol* 1994;45(6):1227-34.

41. Veh RW, Lichtinghagen R, Sewing S, et al. Immunohistochemical localization of five members of the Kv1 channel subunits: contrasting subcellular locations and neuron-specific co-localizations in rat brain. *Eur J Neurosci* 1995;7(11):2189-205.
42. Fadool DA, Tucker K, Perkins R, et al. Kv1.3 channel gene-targeted deletion produces "Super-Smeller Mice" with altered glomeruli, interacting scaffolding proteins, and biophysics. *Neuron* 2004;41(3):389-404.
43. Cornblath DR, Bienen EJ, Blight AR. The safety profile of dalfampridine extended release in multiple sclerosis clinical trials. *Clin Ther* 2012;34(5):1056-69.
44. Goodman AD, Brown TR, Edwards KR, et al. A phase 3 trial of extended release oral dalfampridine in multiple sclerosis. *Ann Neurol* 2010;68(4):494-502.
45. Pennington MW, Beeton C, Galea CA, et al. Engineering a stable and selective peptide blocker of the Kv1.3 channel in T lymphocytes. *Mol Pharmacol* 2009;75(4):762-73.
46. Matheu MP, Beeton C, Garcia A, et al. Imaging of effector memory T cells during a delayed-type hypersensitivity reaction and suppression by Kv1.3 channel block. *Immunity* 2008;29(4):602-14.
47. Darger B, Gonzales N, Banuelos RC, et al. Outcomes of Patients Requiring Blood Pressure Control Before Thrombolysis with tPA for Acute Ischemic Stroke. *The western journal of emergency medicine* 2015;16(7):1002-6.
48. Huang W, Qiu C, von Strauss E, et al. APOE genotype, family history of dementia, and Alzheimer disease risk: a 6-year follow-up study. *Archives of neurology* 2004;61(12):1930-4.
49. Braak H, Braak E. Staging of Alzheimer's disease-related neurofibrillary changes. *Neurobiology of aging* 1995;16(3):271-8; discussion 8-84.
50. Shrout PE, Fleiss JL. Intraclass correlations: uses in assessing rater reliability. *Psychological bulletin* 1979;86(2):420-8.
51. Schneider CA, Rasband WS, Eliceiri KW. NIH Image to ImageJ: 25 years of image analysis. *Nat Methods* 2012;9(7):671-5.
52. Pannasch U, Farber K, Nolte C, et al. The potassium channels Kv1.5 and Kv1.3 modulate distinct functions of microglia. *Mol Cell Neurosci* 2006;33(4):401-11.
53. Wang Y, Cella M, Mallinson K, et al. TREM2 lipid sensing sustains the microglial response in an Alzheimer's disease model. *Cell* 2015;160(6):1061-71.
54. Freilich RW, Woodbury ME, Ikezu T. Integrated expression profiles of mRNA and miRNA in polarized primary murine microglia. *PloS one* 2013;8(11):e79416.
55. Menteyne A, Levavasseur F, Audinat E, et al. Predominant functional expression of Kv1.3 by activated microglia of the hippocampus after Status epilepticus. *PloS one* 2009;4(8):e6770.
56. Liu J, Xu P, Collins C, et al. HIV-1 Tat protein increases microglial outward K(+) current and resultant neurotoxic activity. *PloS one* 2013;8(5):e64904.
57. Peng Y, Lu K, Li Z, et al. Blockade of Kv1.3 channels ameliorates radiation-induced brain injury. *Neuro Oncol* 2014;16(4):528-39.

G. TABLES

Table 1. Baseline characteristics of study population

Variable	Measure	AD (n=10)	Non-AD controls (n=10)
Age	Years (mean± SD)	71.6±11.1	71.5±11.9
Sex	Female (%)	4, 40%	4, 40%
ApoE allele			
4/4	N, %	3, 30%	0, 0%
4/3	N, %	5, 50%	1, 1%
3/3	N, %	2, 20%	6, 60%
2/3	N, %	0, 0%	3, 30%
Race (Caucasian)	Caucasian, %	9, 90%	8, 80%
Braak Stage (N, %)			
0	N, %	0, 0%	1, 10%
I	N, %	0, 0%	0, 0%
II	N, %	0, 0%	9, 90%
III	N, %	0, 0%	0, 0%
IV	N, %	0, 0%	0, 0%
V	N, %	0, 0%	0, 0%
VI	N, %	10, 100%	0, 0%

[#]Braak stage is a neuro-pathological grading system based on amount and spread of plaques and tangles in the AD brain. Stage 0 indicates no plaques or tangles while VI indicates severe disease with extensive cortical involvement.

* p-value < 0.05 for Fisher Exact test. For ApoE allele status, proportion of patients with at least one ApoE4 allele were compared in AD and non-AD groups. For Braak stage, proportion of patients with stage III-VI were compared between AD and non-AD groups.

Table 2. Comparison of Kv1.3 and Iba1 immunostaining intensity and density in frontal cortex of AD and non-AD post-mortem brain samples.

Variable	AD (n=10)	Non-AD (n=10)	p-value*
Kv1.3			
Mean Staining Intensity (SD)	2.03 (0.75)	1.27 (0.71)	
Median Staining Intensity (IQR)	2.25 (1.6-2.5)	1.42 (0.67-1.8)	0.029
Mean Immunostaining Density (SD)	2.27 (0.82)	1.48 (0.82)	
Median Staining Density (IQR)	2.5 (1.83-2.63)	1.5 (0.83-2.25)	0.023
IBA-1	**AD (n=10)**	**Non-AD (n=10)**	**p-value**
Mean Immunostaining Intensity (SD)	2.83 (0.24)	2.40 (0.64)	
Median Staining Intensity (IQR)	3 (2.67-3)	2.5 (1.67-3.0)	0.17
Mean Immunostaining Density (SD)	2.72 (0.42)	1.97 (0.53)	
Median Staining Density (IQR)	3 (2.5-3.0)	2.00 (1.67-2.33)	0.004

Kv1.3 staining intensity and density was calculated as the average of readings by two blinded independent observers. Six cortical regions were graded by each observer. Standard deviation (SD) of mean and interquartile range (IQR) for the median values is shown. Iba1 is a well characterized marker of microglia used for immunohistochemical analyses. * p-value calculated based on the non-parametric Mann-Whitney U test comparing 2 groups.

H. FIGURES

Figure 1. Kv1.3 channel expression by M1 and M2 microglia

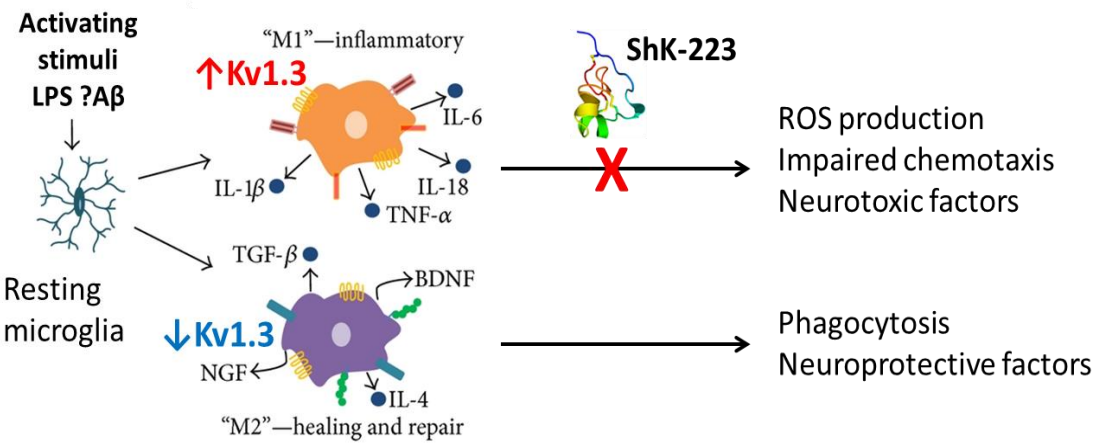

Pro-inflammatory M1 microglia activated by lipopolysaccharide (LPS) or other stimuli including Aβ upregulate Kv1.3 channels while protective M2 microglia do not. Markers of M1 (IL1B, IL18, TNF alpha, IL6) and M2 microglia (TGF beta, BDNF, NGF) are shown in the figure. Pro-inflammatory and neurotoxic effects of M1 microglia are likely to be inhibited by Kv1.3 channel blockers such as ShK-223.

Figure 2. Higher Kv1.3 and Iba1 expression in AD frontal cortex compared to non-AD controls

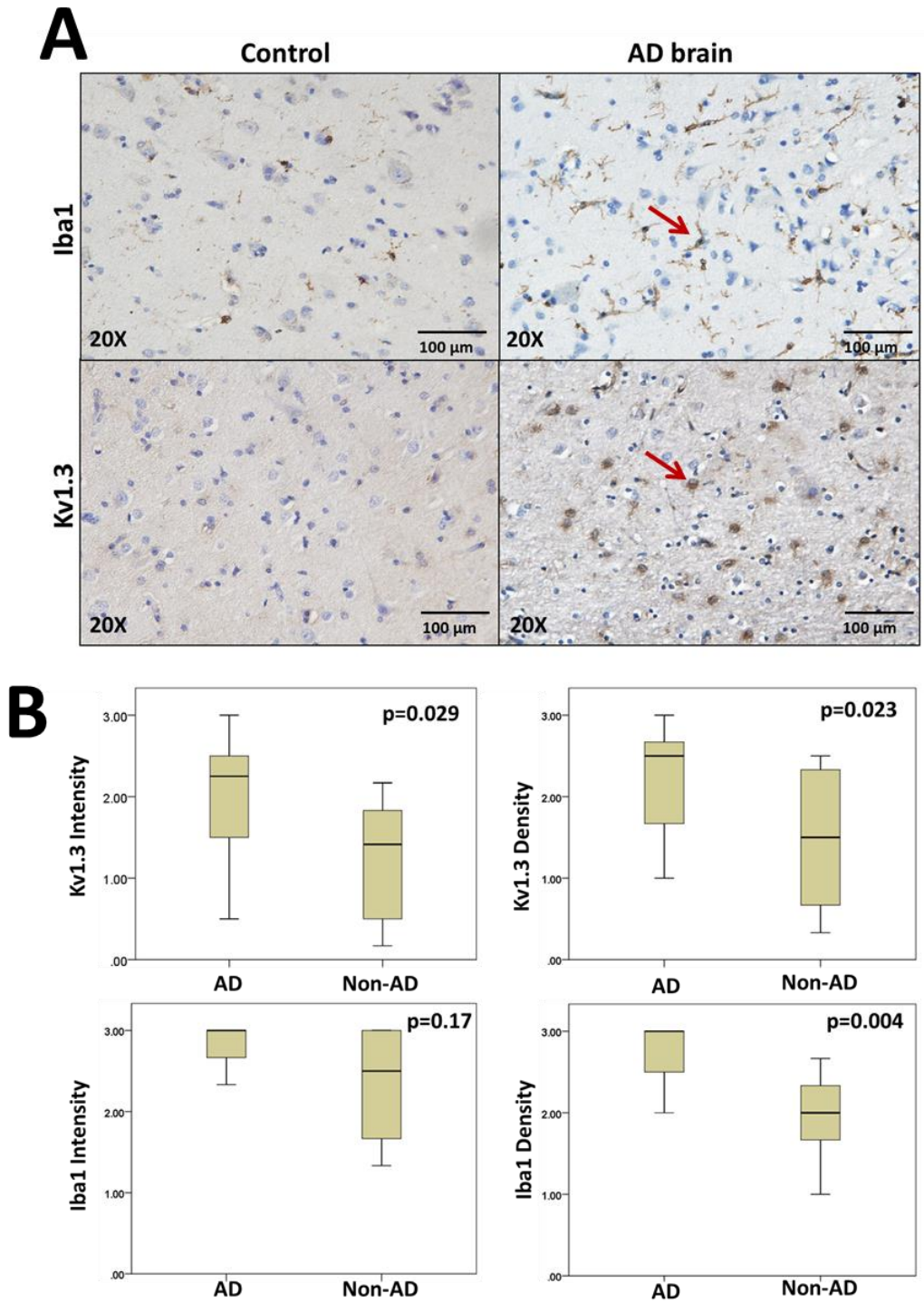

Representative images from AD and non-AD control cases showing increased microglial Iba1 positivity along with increased Kv1.3 positive cells. Blue: Nuclear stain, Brown represents Iba1 in the upper panel and Kv1.3 in the lower panel. **(B)** Box-plots from data acquired an immunohistochemistry study from 10 AD and 10 non-AD age (±5yrs) and gender-matched post-mortem brain specimens all with post-mortem interval <12 hours. Kv1.3 staining intensity and density and Iba1 staining intensity and density are presented. P-values represent results from Mann-Whitney U tests comparing median values across AD and non-AD groups (alpha level 0.05).

Figure 3. Increased Kv1.3 expression in hippocampal cortex in AD brain by an image analysis approach.

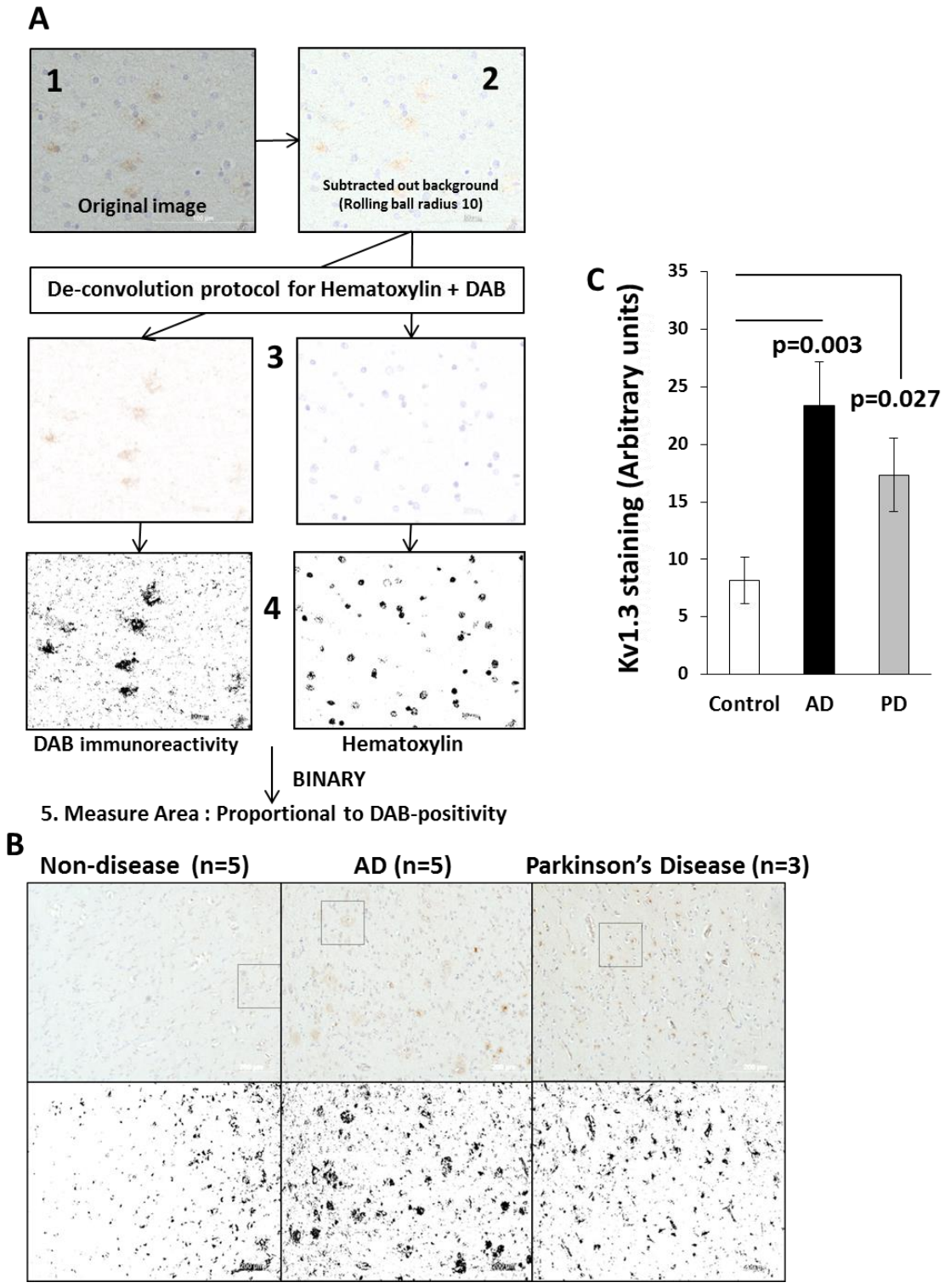

Figure 3 (A) Five steps involved in image processing and analytic approach for objective image-analysis using Image J software and the deconvolution plugin. ImageJ deconvolution plugin was downloaded from *http://imagej.nih.gov/ij/plugins/fftj.html*. **(B)** Kv1.3 expression was assessed in a blinded manner in 5 AD, 5 non-disease and 3 Parkinson's disease brain samples from the hippocampal cortex. Each image was de-convoluted using ImageJ and the area of DAB-positivity was calculated. Three images per sample were used for analysis. Upper panel shows the original acquired images and panel below shows the images for Kv1.3 immunostaining after deconvolution. **(C)** Quantification and comparison of Kv1.3 staining performed using the Mann-Whitney U test (alpha level 0.05) used for pairwise statistical comparisons.

Figure 4. Western-Blot confirmation of increased Kv1.3 channel protein expression in AD brain compared to non-AD controls.

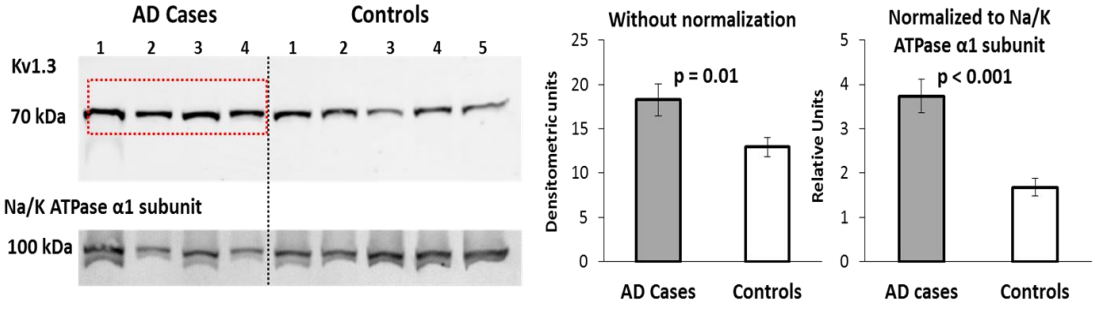

Western-Blot confirmation of increased Kv1.3 channel protein expression in AD brain compared to non-AD controls. Anti-Kv1.3 antibody detected the protein of interest (70 kilo Dalton size) by Western Blot analysis in 4 AD and 5 non-AD post-mortem human frontal cortex samples. Non-normalized and normalized Kv1.3 protein levels were statistically higher in AD as compared to non-AD control samples. 2-tailed independent sample T test assuming equal variances was performed for comparison.

Figure 5. Kv1.3 channels in AD cortex are restricted to Iba1 positive microglia

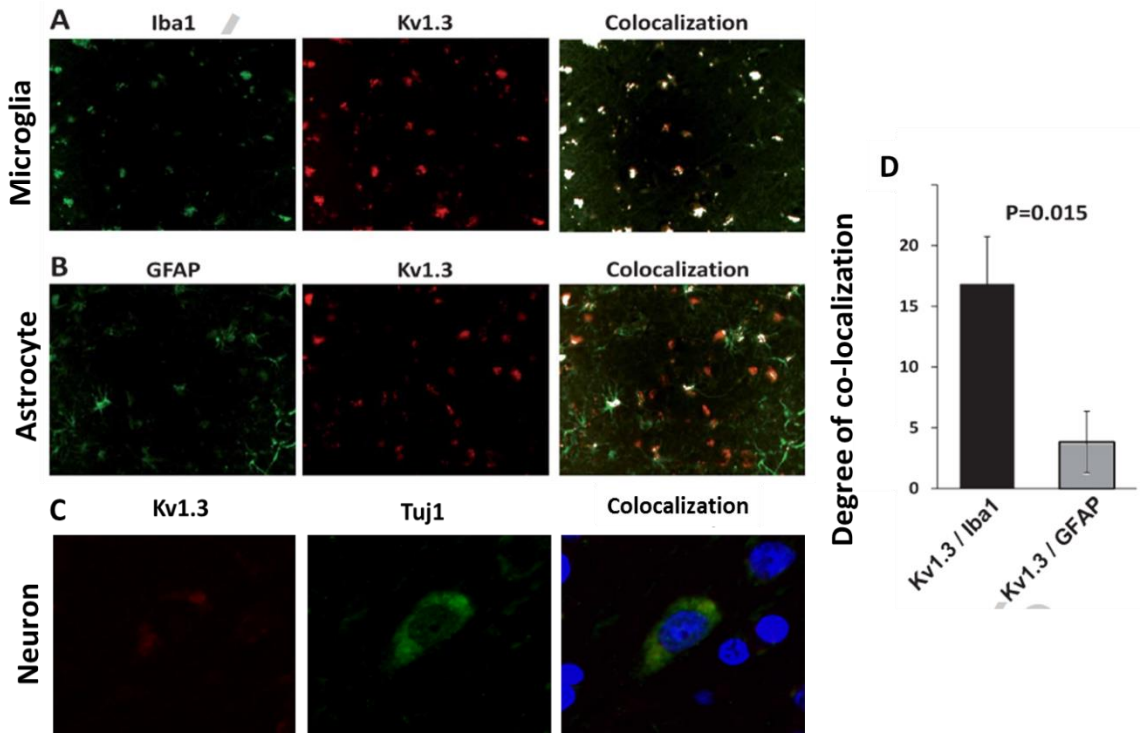

In human AD frontal cortical sections, Kv1.3 channel expression (Red) was found to highly co-localize with Iba1, a pan-microglial marker **(A)**. On the other hand, Kv1.3 co-localized only to minimally co-localize with astrocyte marker GFAP **(B)** and did not co-localize with neuronal marker Tuj-1 **(C)**. Nuclear staining shown in Blue. Quantification of co-localization was performed using Image J software and degree of co-localization was calculated based on the number of colored pixels per image that were positive for the red and/or green channel. Three AD samples were used and at least 5 images were acquired per sample. Mean degree of co-localization between Kv1.3 and Iba1 and between Kv1.3 and GFAP was calculated and compared using a 2-tailed T-test assuming equal variance.

Figure 6. Kv1.3 expression by microglia is abundant in the vicinity of Aβ plaques in the human AD brain.

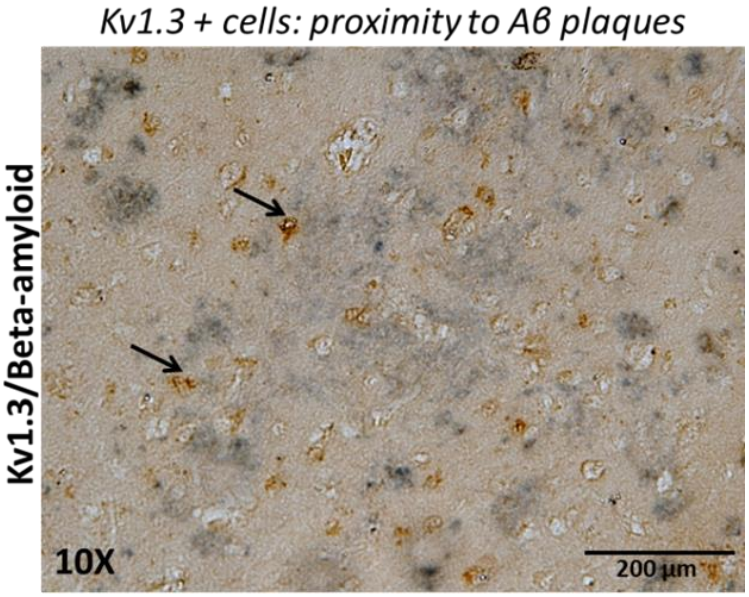

Three AD frontal cortical sections were double immunostained with anti-Kv1.3 (brown, arrows) and anti-Aβ (black) antibodies. A representative image shown demonstrates that Kv1.3 positive glial cells are most abundant around Aβ positive plaques.

Figure 7. High affinity and specificity of anti-Kv1.3 antibody for Kv1.3 channel protein in immunohistochemistry.

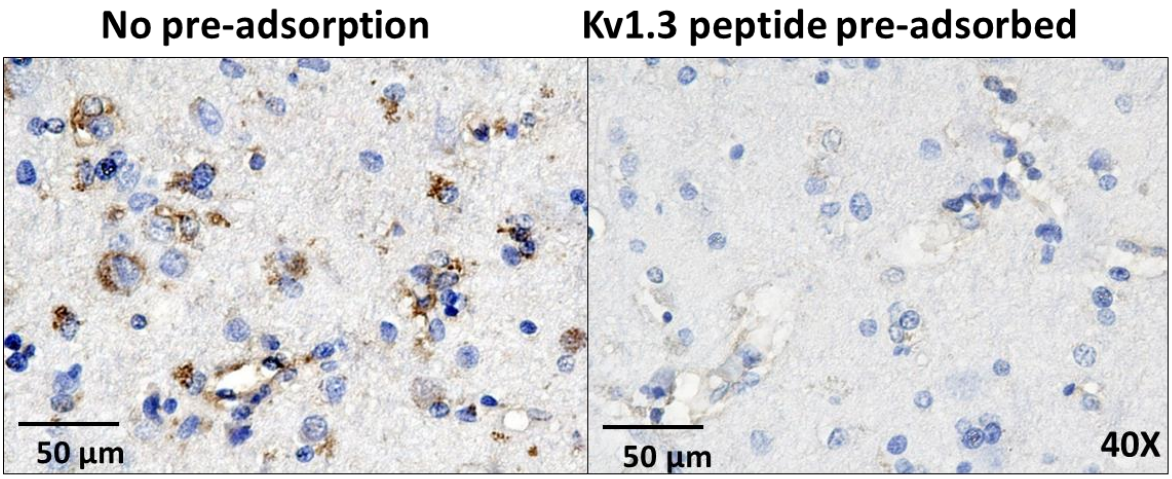

Anti-Kv1.3 antibody at 1:100 dilution was incubated with saturating concentrations of the immunizing Kv1.3 peptide. This pre-adsorbed reagent was then used for immunostaining experiments. Pre-adsorption with the immunizing peptide should abolish any immunostaining if the antibody specifically recognizes Kv1.3 with high affinity and specificity. As predicted, pre-adsorption abolished all Kv1.3 immunoreactivity from the AD brain. Kv1.3 staining shown in brown. Nuclear stain shown in Blue.

Figure 8. Kv1.3 channel blockade abolishes Aβ42-induced ROS production by BV2 microglia.

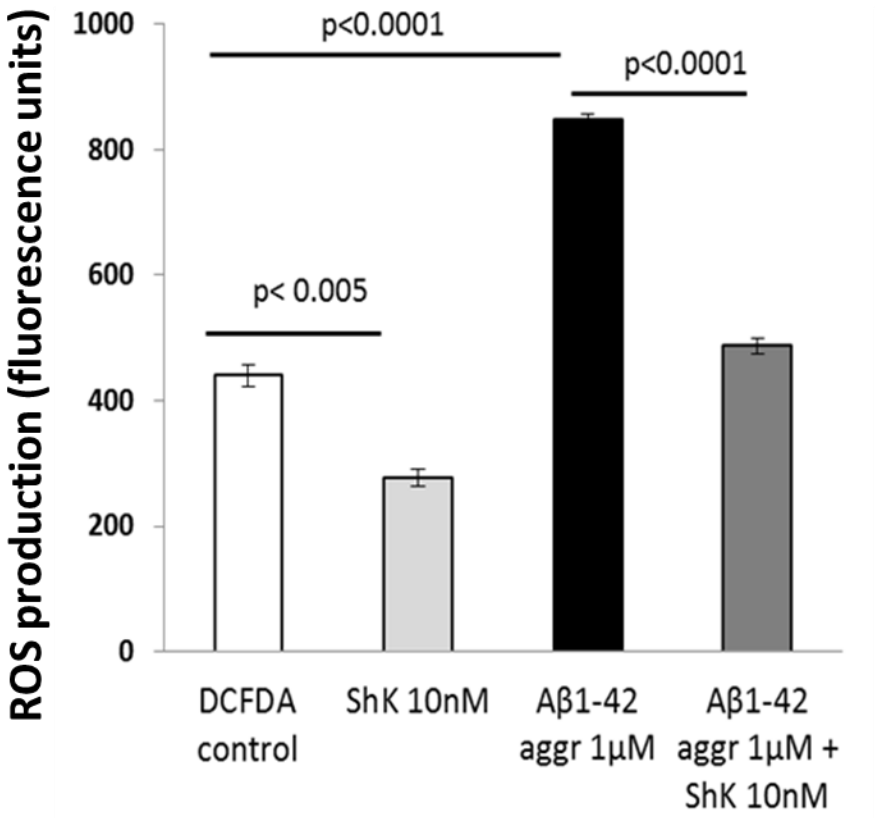

In the DCFDA assay of ROS production in-vitro, we found that Aβ42 induced significantly higher ROS levels as compared to control treatments. ShK-223, a hihgly selective Kv1.3 channel blocker at 10 nM concentrations did not increase ROS production by itself, but significantly inhibited Aβ42-induced ROS production. P-values shown are for pairwise comparisons of ROS production using two-tailed independent sample T tests at alpha level of 0.01, assuming equal variances. Overall one-way ANOVA was highly statistically significant ($p<0.0001$, F-statistic 1929, Df=3). Mean ROS production is shown with error bars representing one SD.

Figure 9. Figure 9. LPS-mediated and Aβ42-mediated inhibition of microglial gap closure is partly reversed by Kv1.3 channel blockade by ShK-223.

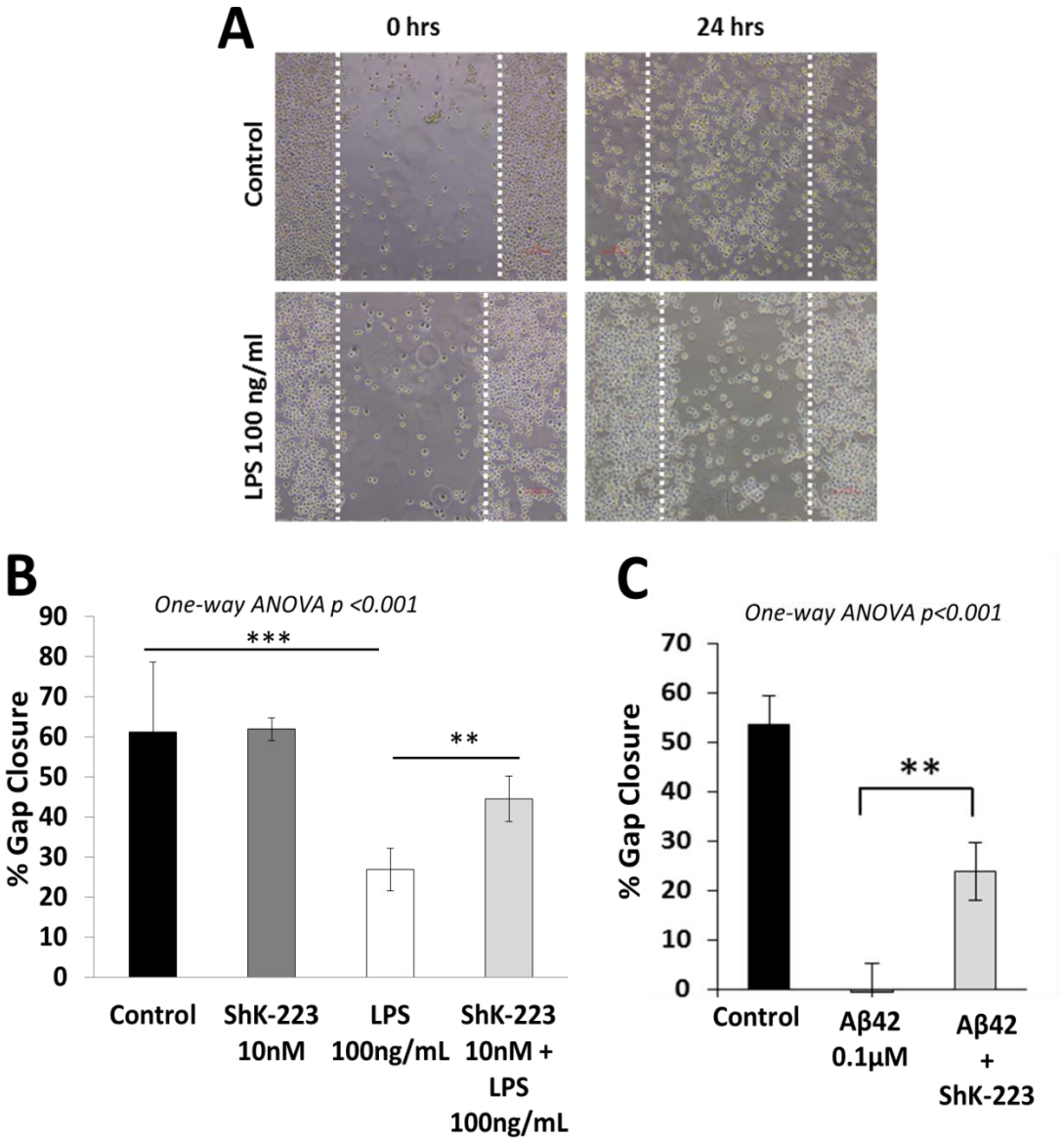

(A) Representative example of LPS-induced inhibition of gap closure by BV2 microglia. A scratch in a nearly confluent microglial culture plate is placed with a 200 μL pipette tip (gap shown between white dotted lines). After 24 hours, this gap is closed by migrating microglia. LPS

treatment at the time of scratch placement inhibits the ability of microglia to close this gap at 24 hours. **(B)** LPS-induced inhibition of gap closure was partly reversed by ShK-223 treatment without any direct toxic effect of ShK-223. **(C)** Similar to LPS, Aβ42 also inhibited gap closure but more profoundly. This effect was also partly reversed by ShK-223 treatment at the time of scratch placement. Mean percentage gap closure for each condition is shown with error bars representing one SD. *** $p<0.005$, **$p<0.01$ for pairwise comparisons of mean percentage gap closure using independent sample 2-tailed T test assuming equal variance.